Journal of
*Manufacturing and Materials Processing*

MDPI

*Article*

# Hydrophobic Material: Effect of Alkyl Chain Length on the Surface Roughness

**Alfa Akustia Widati [1,2,*], Mochamad Zakki Fahmi [1,2], Satya Candra Wibawa Sakti [1,2], Titah Aldila Budiastanti [1] and Tri Esti Purbaningtias [3]**

[1] Department of Chemistry, Faculty of Science and Technology, Universitas Airlangga, Surabaya 60115, Indonesia
[2] Supramodification and Nano-Micro Engineering Research Group, Universitas Airlangga, Surabaya 60115, Indonesia
[3] Chemical Analysis Program, Faculty of Mathematics and Natural Sciences, Universitas Islam Indonesia, Yogyakarta 55584, Indonesia
* Correspondence: alfaakustia@fst.unair.ac.id

**Abstract:** The clean technologies of self-cleaning surfaces are expanding rapidly. Highly hydrophobic coatings with strong adhesion, high durability, and dirt-free surfaces have been prepared via sol-gel deposition of $SiO_2$-$TiO_2$-alkylsilane. The influence of the effects of the alkyl chain length of silane on surface roughness was investigated. This deposition involved a one-layer technique to produce the rough surfaces. The bimetal oxide of $SiO_2$-$TiO_2$ created a high level of surface roughness. As a result, the water contact angle of the coatings increased with the increasing alkyl chain length of silane (up to C=8). However, the water contact angle decreased when the C=16 of alkylsilane was applied. It was predicted that the longer alkyl chain would cause the molecules to collapse. The higher hydrophobicity was produced by $SiO_2$-$TiO_2$-OTMS coatings with a water contact angle of about 140.67 ± 1.23°. The effect of the dip-coating technique (one layer and layer-by-layer) on hydrophobicity was also discussed. The results showed that coatings produced by the one-layer technique had a higher contact angle than coatings made by the layer-by-layer technique. The coatings were stable under outdoor exposure and able to hinder dirt attachment to their surfaces.

**Keywords:** clean technologies; self-cleaning; hydrophobic; alkyl chain length; $SiO_2$-$TiO_2$-alkylsilane



**Citation:** Widati, A.A.; Fahmi, M.Z.; Sakti, S.C.W.; Budiastanti, T.A.; Purbaningtias, T.E. Hydrophobic Material: Effect of Alkyl Chain Length on the Surface Roughness. *J. Manuf. Mater. Process.* **2022**, *6*, 110. https://doi.org/10.3390/jmmp6050110

Academic Editor: Steven Y. Liang

Received: 28 July 2022
Accepted: 18 September 2022
Published: 28 September 2022



## 1. Introduction

Hydrophobic materials are widely used for self-cleaning surfaces. Self-cleaning is the ability of coatings to clean their surface by themselves. Hydrophobic coatings perform a self-cleaning action through the formation of spherical water droplets that readily roll away from the surface, carrying the dirt with them. The different mechanisms of hydrophobic self-cleaning were revealed on hydrophobic, highly hydrophobic, and superhydrophobic coatings [1]. In other words, the water contact angle greatly influences the performance and mechanism of self-cleaning properties.

The highest self-cleaning efficiency was observed on the superhydrophobic surface, which was prepared using TEOS, polydimethylsiloxane, and nanosilica. The dirt accumulated on the superhydrophobic surfaces at about 34.99% and decreased to 4.13% after the cleaning process. Air was trapped on the superhydrophobic surface [2]. This trapped air reduced the contact area between the water droplet and the surface. The water droplets easily rolled off the surface due to the low water adhesion properties of the surface. Therefore, no dirt remained on the surface [3].

Hydrophobicity is influenced by surface energy and surface roughness. Based on the Young equation, the highest contact angle will be achieved with the lowest surface energy and highest surface roughness. Fluorosilane presents the lowest surface energy. Unfortunately, it is classified as a toxic compound [4,5]. Recently, researchers have been

considering the replacement of fluorosilane with alkylsilane. As we know, the surface energy of alkylsilane is higher than fluorosilane, therefore it must be modified with a rough surface to achieve high hydrophobicity. This roughness is achieved by etching, sol-gel, electrochemical deposition, chemical grafting, chemical vapor deposition, and nanoparticle deposition [6].

Superhydrophobic glass was successfully produced by the deposition of $SiO_2$ and alkylsilane [7–10]. More than one alkylsilane was needed to decrease the surface energy. Consequently, it created greater thickness and caused lower adhesion between the coatings and the glass substrate [11]. In other words, although superhydrophobic glass was achieved, there were still limitations to the adhesion of coatings, as reported by Liu et al. [12]. In practical applications, the main criterion for the acceptable performance of coated materials is the bonding strength of the coating to the substrate. Some researchers have reported ways to overcome this problem, such as adding $SiO_2$ sol to increase the amount of the hydroxyl group, using $SiO_2$-$TiO_2$ composite, applying a dip coating method, and the sol-gel deposition technique [2,7,13,14].

For this research, we fabricated highly hydrophobic glass and enhanced the adhesion strength by coating the glass using $SiO_2$, $TiO_2$, and one alkylsilane via sol-gel deposition. The effects of long-chain alkylsilane on the hydrophobicity of coated glass have been investigated. Three alkylsilanes with different chain lengths were studied: methyltrimethoxysilane (MTMS, C=1), octyltrimethoxysilane (OTMS, C=8), and hexadecyltrimethoxysilane (HDTMS, C=16). Spataru and co-workers [15] reported that samples containing long hydrocarbon chains are highly hydrophobic. The increase in the hydrocarbon chain length contributed to higher non-polar properties in the $CH_3$ groups. However, Tang and colleagues [16] stated that the short alkyl chain of silane exhibited a high water-contact angle. The surface coupling of the short alkyl chain of silane and the vertical polymerization (intermolecular silane coupling) created thick films with micro-nanoscale roughness. We also discuss the influence of dip-coating techniques (both layer-by-layer and one-layer). Our research also studied the self-cleaning performance of samples. Our results show that coated glass with $SiO_2$-$TiO_2$-OTMS displays the highest hydrophobicity. Interestingly, the as-prepared glass exhibits unique properties when a self-cleaning test is applied. The coated glass hinders the dirt's attachment to the surface; therefore, water is not required to clean the surface.

## 2. Materials and Methods

### *2.1. Materials*

Tetraethylorthosilicate (TEOS, 99%) and titanium tetraisopropoxide (TTIP, 97%) as the $SiO_2$ and $TiO_2$ precursor, were purchased from Sigma Aldrich, St. Louis, MO, USA. Methyltrimethoxysilane (MTMS, 95%), octyltrimethoxysilane (OTMS, 96%), and hexadecyltrimethoxysilane (HDTMS, 85%) as the hydrophobic modifier were obtained from TCI Chemicals, Tokyo. Glacial acetic acid (100%) as acid catalyst was purchased from Merck, Rahway, NJ, USA. Absolute ethanol was purchased from JT Baker, Princeton, NJ, USA. All these materials were used as received without any further purification. Glass slides ($38 \times 12 \times 1$ mm) were used as a substrate.

### *2.2. Preparation of Acid-Catalyzed $SiO_2$-$TiO_2$-Alkylsilane Sol*

$SiO_2$-$TiO_2$-MTMS sol was fabricated by mixing $SiO_2$, $TiO_2$, and MTMS sols. $SiO_2$, $TiO_2$, and MTMS sols were prepared in separate containers. First, 7.5 mmol of $SiO_2$ sol was prepared by mixing 1.67 mL of TEOS in 4 mL of ethanol. Then, 7.5 mmol of $TiO_2$ sol was made by mixing 2.22 mL of TTIP with 4 mL of ethanol. Then, 15 mmol of MTMS sol was prepared by adding 2.1 mL of MTMS into 4 mL of ethanol. In all sols, the pH was adjusted to pH 2 with the addition of glacial acetic acid. Each sol was further stirred for 60 min at 70 °C. After that, the $SiO_2$ and $TiO_2$ sols were mixed and stirred continuously for 60 min at 70 °C. The MTMS sol was then added to the $SiO_2$-$TiO_2$ sol. The sol was then stirred and heated at 70 °C until the volume was 20 mL.

The effects of the $SiO_2$, $TiO_2$, and MTMS sols on hydrophobization were studied by varying the mol value. The various amounts of $SiO_2$, $TiO_2$, and alkylsilane were 3.75, 7.5, 15, and 30 mmol, respectively. While the mol of $SiO_2$ was varied, we kept the mols of $TiO_2$ and MTMS constant. The optimum mol of $SiO_2$ and the constant mol of MTMS were handled to investigate the influence of the amount of $TiO_2$. The variation in MTMS mol was studied using the optimum mols of $SiO_2$ and $TiO_2$.

The influence of the alkyl chain length of silane was investigated using $SiO_2$-$TiO_2$-MTMS, $SiO_2$-$TiO_2$-OTMS, and $SiO_2$-$TiO_2$-HDTMS sols. The preparation procedures of these sols were similar to previously described methods used in the preparation of $SiO_2$-$TiO_2$-MTMS.

### *2.3. Preparation of Coatings*

The glass substrates were cleaned with ultrasonication in ethanol for 30 min. The cleaned glass was then immersed in the coating solutions, with a withdrawal speed of 3 cm/min. The one-layer coating technique was conducted using $SiO_2$, $TiO_2$, and alkylsilane, prepared in one vessel. After immersion of the glass in the coating solution, the coated glass substrates were firstly dried at room temperature (33 °C) for 10 min and then at 70 °C for 30 min.

In the layer-by-layer deposition, the $SiO_2$, $TiO_2$, and alkylsilane sols were prepared separately. $SiO_2$, $TiO_2$, and alkylsilane were employed as the bottom, middle, and top layers. Each layer was cured at room temperature (33 °C) for 10 min, and then followed at 70 °C for 30 min. The one-layer technique was formed as a one-time coating onto the substrates. Meanwhile, the layer-by-layer technique was applied in three layers, wherein $SiO_2$, $TiO_2$, and alkylsilane were deposited one by one. This means that the first, second, and third layers were $SiO_2$, $TiO_2$, and alkylsilane, respectively.

### *2.4. Characterization*

The contact angle of the coated glasses was measured via ImageJ software (V.1.8.0, Bharti Airtel Ltd) using the drop analysis–drop snake method. The types of chemical bonds were identified using Fourier transform infrared spectroscopy (Shimadzu IR-Tracer 100, Europe). The spectrum was recorded in the wavenumber range of 4000–400 $cm^{-1}$. The surface topography and roughness value of the samples were measured using atomic force microscopy (N8 Neos Bruke, Herzogenrath, Germany) in the non-contact mode under ambient conditions. The morphology of the surfaces was studied using scanning electron microscopy (Carl Zeiss EVO MA 10, Oberkochen, Germany). The cross-cut adhesion test according to ASTM D3359 was employed to determine the adhesion quality of the coatings. The stability of coatings was studied by measuring the change in water contact angle under outdoor exposure for one month, with a relative humidity of between 38 and 76% and a temperature of between 23 and 35 °C.

### *2.5. Anti-Dirt Test*

The performance of the samples' anti-dirt properties was evaluated using $CuCl_2.2H_2O$ as artificial dirt. The choice of $CuCl_2.2H_2O$ was adopted from previous research [17]. The coated glass was spiked with $CuCl_2{\cdot}2H_2O$ and was then weighed ($m_1$). The glass was then placed in an inclined position. Water was then dripped slowly onto the top side of the glass. After that, the glass was re-weighed ($m_2$) to determine the amount of $CuCl_2{\cdot}2H_2O$ that was still left on the surface. The amount of $CuCl_2{\cdot}2H_2O$ remaining was calculated using Equation 1. The less $CuCl_2{\cdot}2H_2O$ there was on the surface, the better the self-cleaning properties of the glass. As a control, a self-cleaning test was also carried out on the uncoated glass.

$$\text{The amount of remaining dirt on the surface } (\%) = \frac{m_2}{m_1} \times 100\% \quad (1)$$

## 3. Results and Discussion

### 3.1. Wetting Properties of Coatings with Various Compositions of $SiO_2$ and $TiO_2$

$TiO_2$ plays a major role in the wettability of surfaces. The hydrophobic surfaces that were prepared using amorphous $TiO_2$ presented a stable water-contact angle. The $TiO_2$ phase of $SiO_2$-$TiO_2$-alkylsilane was investigated using X-ray diffraction (XRD) analysis. The XRD spectra of samples are depicted in Figure 1. All samples showed broad peaks, indicating that the sample had amorphous $TiO_2$. Under UV irradiation, amorphous $TiO_2$ did not demonstrate photocatalytic properties [16]. There were no hydroxyl groups that were released under UV irradiation. As we know, the hydroxyl groups have hydrophilic properties; therefore, this can decrease the contact angle of the coatings.

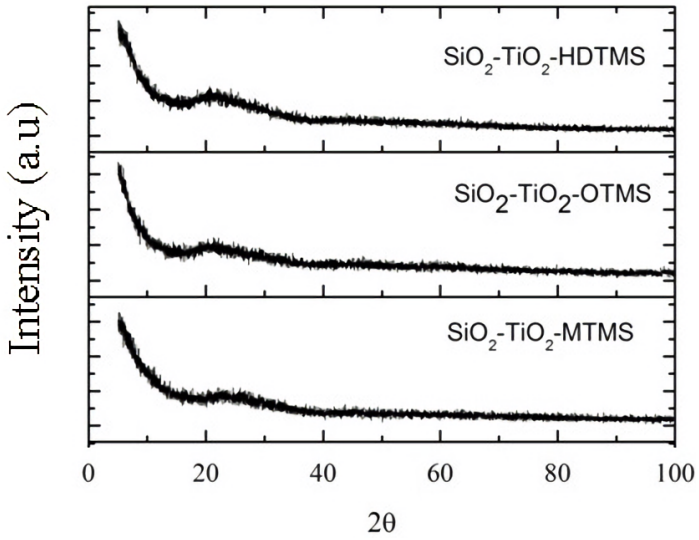


**Figure 1.** The XRD diffractogram of the samples.

Figure 2 shows the contact angle with respect to the $SiO_2$ and $TiO_2$ in the sol. The contact angle increased with increasing $SiO_2$ and $TiO_2$ content from 3.75 to 15 mmol. With $SiO_2$ and $TiO_2$ above 15 mmol, the water contact angle was decreased. These results were influenced by the surface roughness of the coatings. The roughness of the coatings, as measured using SEM, is displayed in Figure 3. Figure 3a–c displays the SEM images of samples using 7.5, 15, and 30 mmol of $SiO_2$. It can be seen that 15 mmol of $SiO_2$ presented a rougher surface than the others. This is because the clustering of $SiO_2$ on the surfaces created rougher surfaces. With $SiO_2$ above 15 mmol, the surface morphology of the coating became smooth. The high content of $SiO_2$ tended to fill the surface holes and create smooth surfaces. A similar trend of topography was also observed for 7.5, 15, and 30 mmol of $TiO_2$ (Figure 3d–f). Comparing the topography of the coatings with various compositions of $SiO_2$ and $TiO_2$, the roughest surface was obtained from the deposition of 15 mmol of $TiO_2$. The agglomeration of particles was clearly obvious. This particle agglomeration resulted in irregular surfaces. According to the data regarding water contact angle and the SEM images, it can be concluded that the rougher the surface is, the higher the hydrophobicity. Table 1 shows the data regarding water contact angle and the roughness value of the samples, which were measured by AFM.

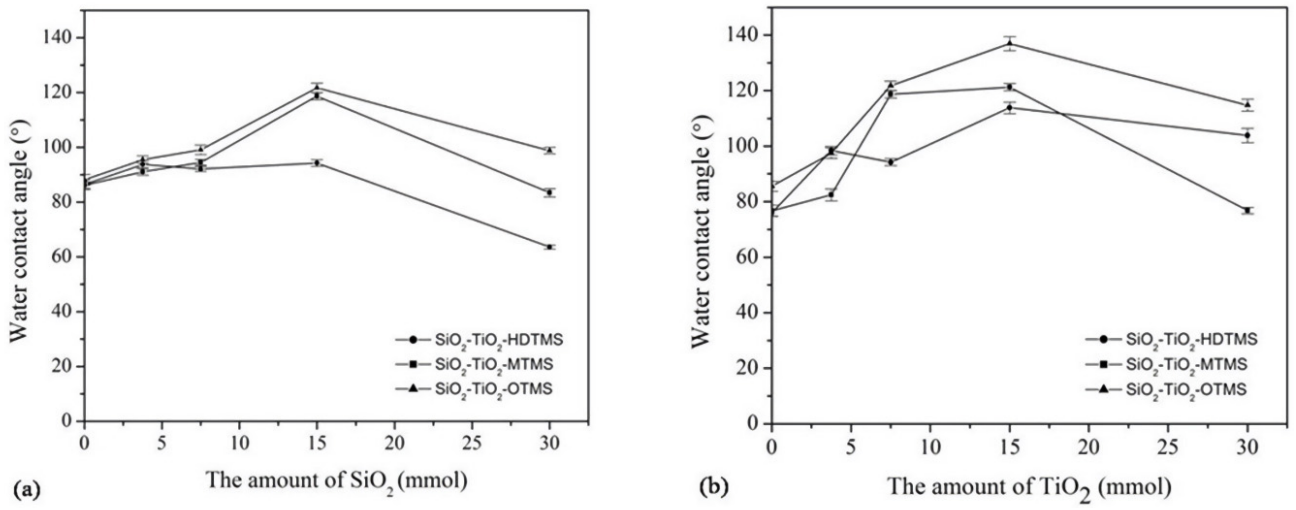


**Figure 2.** Water contact angle of $SiO_2$-$TiO_2$-alkylsilane coatings prepared with various compositions of (**a**) $SiO_2$ (x mmol $SiO_2$, 7.5 mmol $TiO_2$, and 15 mmol alkylsilane) and (**b**) $TiO_2$ (15 mmol $SiO_2$, x mmol $TiO_2$, and 15 mmol alkylsilane).

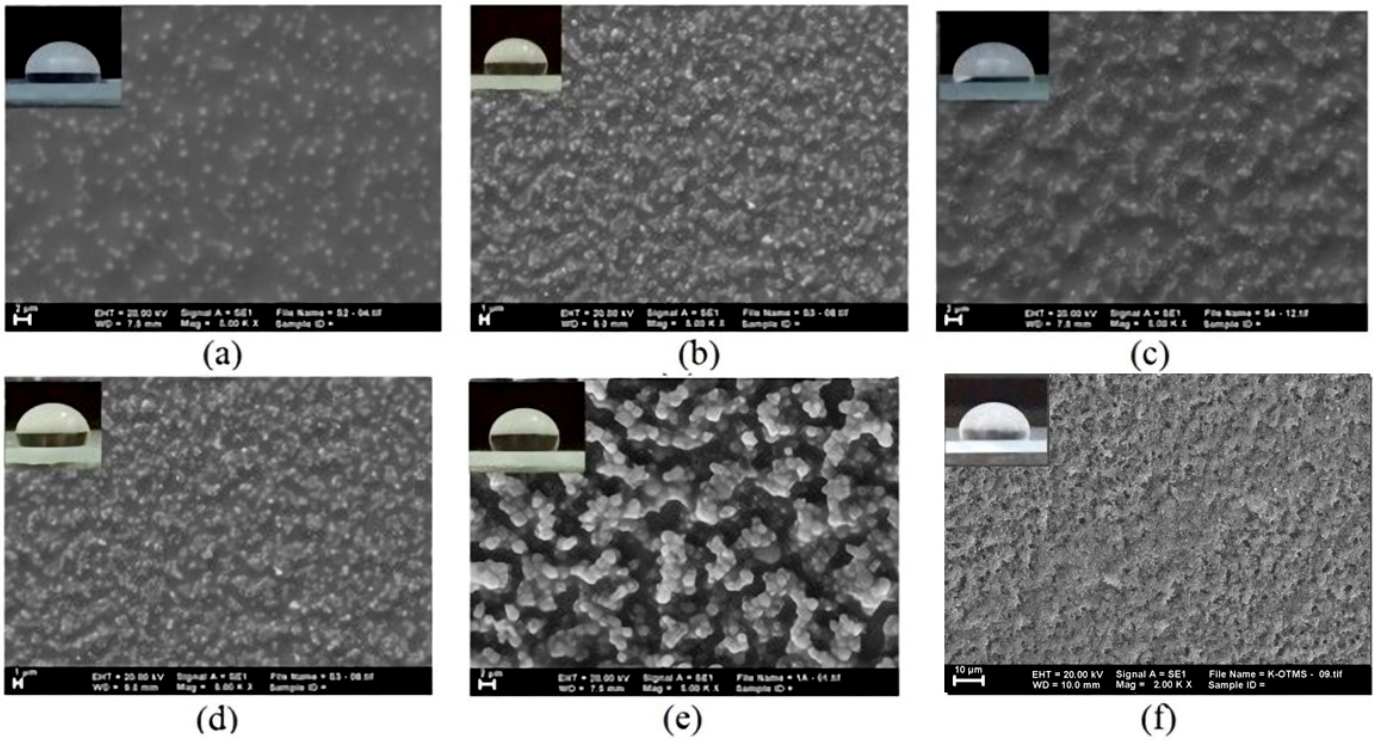


**Figure 3.** The SEM images of $SiO_2$-$TiO_2$-OTMS coatings prepared with (**a**) 7.5, (**b**) 15, and (**c**) 30 mmol of $SiO_2$ (x mmol $SiO_2$, 7.5 mmol $TiO_2$, and 15 mmol OTMS), (**d**) 7.5, (**e**) 15, and (**f**) 30 mmol of $TiO_2$ (15 mmol $SiO_2$, x mmol $TiO_2$, 15 mmol OTMS), respectively.

The decrease in water contact angle in over 15 mmol of $SiO_2$ and $TiO_2$ was also attributed to the increase in the amounts of the hydroxyl groups on the surfaces. The presence of hydroxyl groups enhanced the hydrophilicity of the substrates. We calculated the ratio of peak areas of O-H (~3400 $cm^{-1}$) and C-H (~3400 $cm^{-1}$) vibration in 15 and 30 mmol of $SiO_2$ and $TiO_2$, based on the FTIR data, to quantify the hydroxyl groups on the surface (Figure 4). It was found that 15 mmol of $SiO_2$ and $TiO_2$ had higher $A_{\frac{3400\ cm^{-1}}{1450\ cm^{-1}}}$ values than 15 mmol of $SiO_2$ and $TiO_2$. It means that 15 mmol of $SiO_2$ and $TiO_2$ had higher hydroxyl groups than 15 mmol of $SiO_2$ and $TiO_2$. The abundance of hydroxyl groups on

the surface caused an increase in its hydrophilicity. Table 2 shows the ratio of peak areas of O-H to C-H vibration from the FTIR spectra of $SiO_2$-$TiO_2$-OTMS samples.

**Table 1.** The correlation of water contact angle and roughness value of $SiO_2$-$TiO_2$-OTMS coatings prepared with various $SiO_2$ and $TiO_2$ values.

| Sample | x (mmol) | Water Contact Angle (°) | Roughness Value (nm) |
|---|---|---|---|
| x $SiO_2$, 7.5 mmol $TiO_2$, 15 mmol OTMS | 7.5 | 99.09 ± 1.73 | 11.2 |
| | 15 | 121.75 ± 1.71 | 157 |
| | 30 | 98.79 ± 1.21 | 12.9 |
| 15 mmol $SiO_2$, x $TiO_2$, 15 mmol OTMS | 7.5 | 121.75 ± 1.71 | 163 |
| | 15 | 136.92 ± 2.45 | 235 |
| | 30 | 114.77 ± 2.15 | 87 |

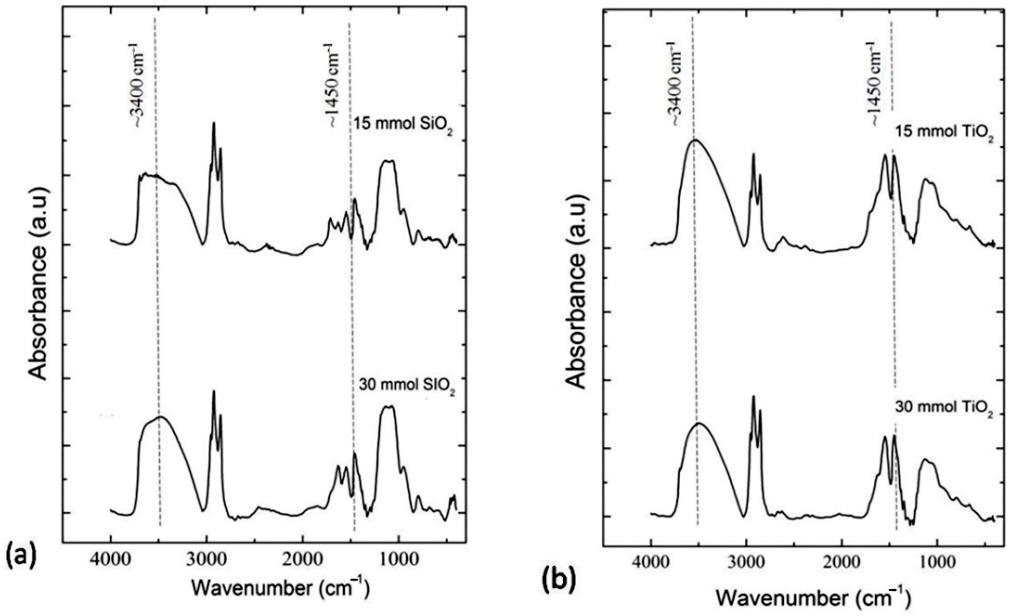


**Figure 4.** The FTIR images of $SiO_2$-$TiO_2$-OTMS coatings prepared with various compositions of (**a**) $SiO_2$ and (**b**) $TiO_2$.

**Table 2.** The ratio of peak areas of O-H to C-H vibration at 3400 and 1450 $cm^{-1}$ from FTIR spectra of $SiO_2$-$TiO_2$-OTMS samples with various compositions of $SiO_2$ and $TiO_2$.

| Sol | Composition (mmol) | The Ratio of Peak Areas (A) at- | | $A_{\frac{3400\ cm^{-1}}{1450\ cm^{-1}}}$ |
|---|---|---|---|---|
| | | 3400 $cm^{-1}$ | 1450 $cm^{-1}$ | |
| $SiO_2$ | 15 | 71.32 | 7.074 | 10.082 |
| | 30 | 42.50 | 4.12 | 10.315 |
| $TiO_2$ | 15 | 64.12 | 12.97 | 4.94 |
| | 30 | 100.47 | 15.85 | 6.33 |

In order to study the effect of $SiO_2$ and $TiO_2$ on hydrophobicity, measurements such as the water contact angle test, AFM analysis, and cross-cut adhesion test were employed. Table 3 reveals the water contact angle of coated glass using $SiO_2$-MTMS, $TiO_2$-MTMS, and $SiO_2$-$TiO_2$-MTMS. It was observed that $SiO_2$-MTMS, $TiO_2$-MTMS, and $SiO_2$-$TiO_2$-MTMS resulted in a water contact angle of about 63.73 ± 1.58°, 80.03 ± 1.45°, and 126.18 ± 1.86°. The use of $SiO_2$-$TiO_2$ produced higher hydrophobicity than others.

**Table 3.** The influence of $SiO_2$, $TiO_2$, and $SiO_2$-$TiO_2$ on the hydrophobicity of coatings.

| Composition (mmol) | | | Water Contact Angle |
|---|---|---|---|
| $SiO_2$ | $TiO_2$ | MTMS | |
| 30 | - | 30 | 63.73 ± 1.58° |
| - | 30 | 30 | 80.03 ± 1.45° |
| 15 | 15 | 30 | 126.18 ± 1.86° |

To address these concerns, we analyzed the topography of $SiO_2$-MTMS, $TiO_2$-MTMS, and $SiO_2$-$TiO_2$-MTMS using AFM as shown in Figure 5. As a result, the topography surface of $SiO_2$-$TiO_2$-MTMS was rougher than $SiO_2$-MTMS and $TiO_2$-MTMS. The roughness values of $SiO_2$-MTMS, $TiO_2$-MTMS, and $SiO_2$-$TiO_2$-MTMS were 4.95, 18.60, and 173 nm, respectively. The average particle sizes of $SiO_2$-MTMS and $TiO_2$-MTMS were 0.472 and 0.175 µm, respectively. The previous research stated that $SiO_2$ resulted in higher particle size than $TiO_2$ under similar conditions [18]. It can be assumed that the difference in particle size between $SiO_2$ and $TiO_2$ led to an increase in the hierarchical morphology.

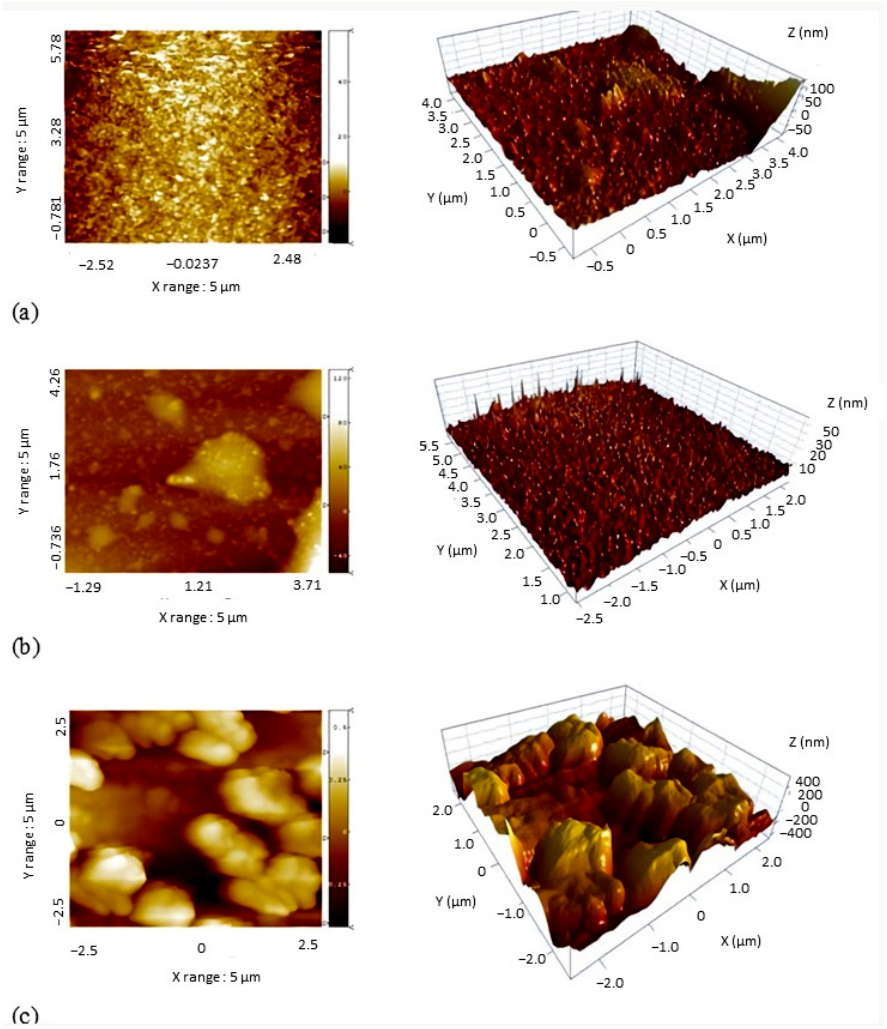


**Figure 5.** The AFM images of (**a**) $SiO_2$-MTMS, (**b**) $TiO_2$-MTMS, and (**c**) $SiO_2$-$TiO_2$-MTMS coatings.

$SiO_2$-$TiO_2$ also improves the adhesion of coatings. The cross-cut adhesion test was conducted with the $SiO_2$-MTMS, $TiO_2$-MTMS, and $SiO_2$-$TiO_2$-MTMS-coated glass. According to ASTM D3359, it was observed that the $SiO_2$-$TiO_2$-MTMS had the highest adhesion of the coating, rated as 4B. Ramirez-Garcia and colleagues also reported that the use of $SiO_2$-$TiO_2$ increased the adhesion of coatings [12].

*3.2. The Influence of Composition and the Alkyl Chain Length of Silane on Hydrophobicity*

Figure 6 displays the water contact angle of coated glass with various compositions of alkylsilane. Both $SiO_2$-$TiO_2$-MTMS and $SiO_2$-$TiO_2$-OTMS show that hydrophobicity increases with an increase in the amount of alkylsilane from 0 to 30 mmol. The decrease in the water contact angle was obtained in 60 mmol of MTMS and OTMS. Moreover, the $SiO_2$-$TiO_2$-HDTMS coatings resulted in an increase in water-contact angle with increasing HDTMS content, from 0 to 15 mmol. In 30 mmol of HDTMS, the water contact angle was reduced. Unfortunately, the observation could not be completed at up to 60 mmol of HDTMS because the sol then changed to a gel. Moreover, the highest contact angle of $140.67 \pm 1.23^{\circ}$ was achieved by those coatings with 15:15:30 mmol of $SiO_2$:$TiO_2$:OTMS.

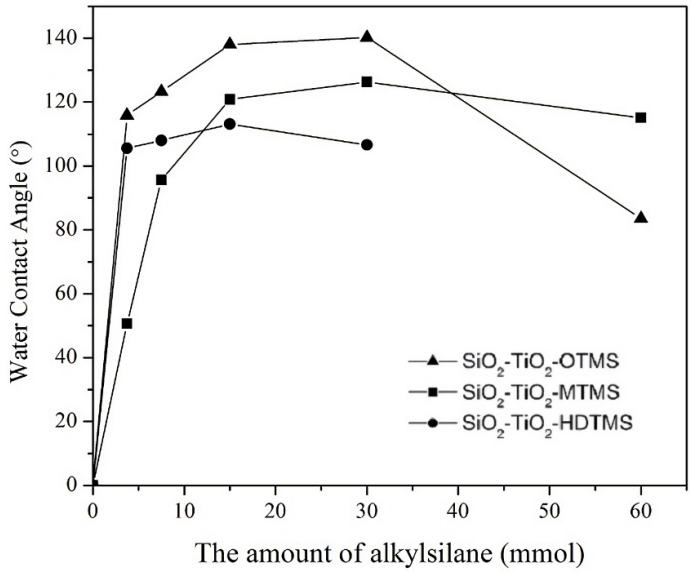


**Figure 6.** The water contact angle of $SiO_2$-$TiO_2$-alkylsilane coatings prepared with various compositions of silane.

The increase in hydrophobicity might be due to the replacement of the polar –OH groups by non-polar $–CH_3$ groups of silane. The FTIR spectra proved this replacement, based on the data of the peak area ratios of O-H to Si-O-Si vibration and C-H to Si-O-Si vibration (Figure 7 and Table 4). There was a decrease in the peak area ratios of O-H to Si-O-Si vibration, which contributed to the decrease in –OH group abundance on the surface. The data also presented an increase in the peak area ratio of C-H to Si-O-Si vibration, which indicated that the number of $–CH_3$ groups on the surface had increased.

**Table 4.** The ratio of peak areas of O-H to Si-O-Si at 3400 and 1100 $cm^{-1}$ and the C-H to Si-O-Si vibration at 1450 and 1100 $cm^{-1}$ from the FTIR spectra of $SiO_2$-$TiO_2$-OTMS samples with various compositions of OTMS.

| Composition (mmol) | The Ratio of Peak Areas (A) at- | | | $A_{\frac{3400\ cm^{-1}}{1100\ cm^{-1}}}$ | $A_{\frac{1450\ cm^{-1}}{1100\ cm^{-1}}}$ |
|---|---|---|---|---|---|
| | **3400 $cm^{-1}$** | **1450 $cm^{-1}$** | **1100 $cm^{-1}$** | | |
| 15 | 108.1 | 18.59 | 32.29 | 3.35 | 0.57 |
| 30 | 93.6 | 18.61 | 40.54 | 2.31 | 0.46 |

The SEM images also revealed that the rougher surfaces were formed by the higher content of alkylsilane (Figure 8). The dispersion of alkylsilane created holes on the surface and tended to produce a hierarchical surface. However, the surface roughness decreased when a larger amount of alkylsilane was applied. The molecules of silane, as predicted, filled the grooves and produced smooth surfaces; therefore, the coatings presented a low contact angle.

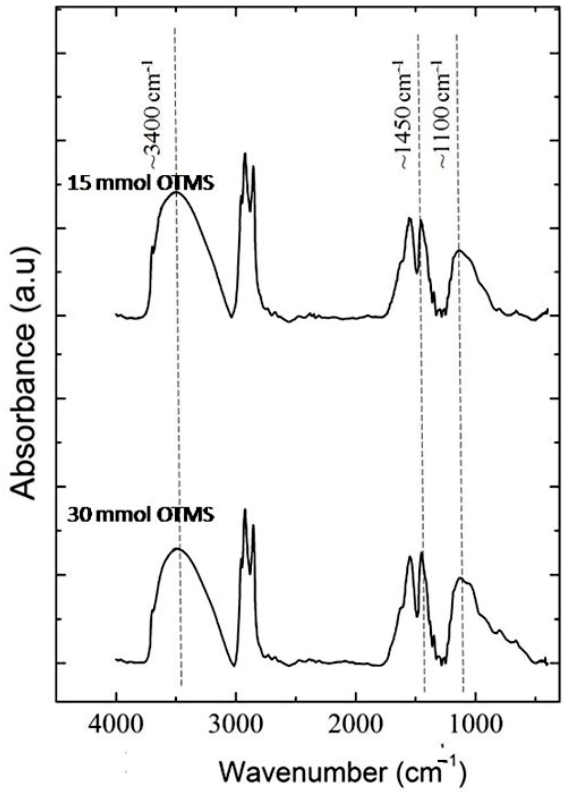


**Figure 7.** The FTIR images of $SiO_2$-$TiO_2$-OTMS coatings, prepared with various compositions of OTMS.

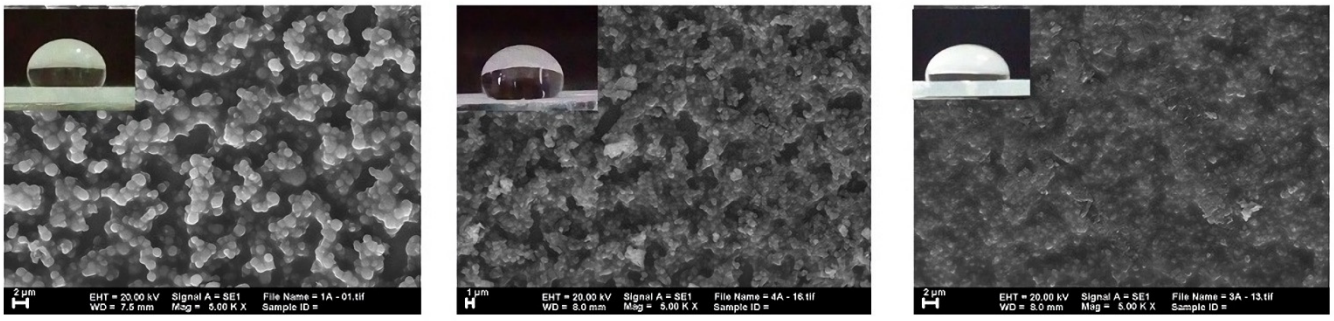


**Figure 8.** The SEM images of $SiO_2$-$TiO_2$-OTMS coatings prepared with (**a**) 15, (**b**) 30, and (**c**) 60 mmol of OTMS.

The main difference between MTMS, OTMS, and HDTMS is the alkyl chain length of silane. The alkyl chain length of MTMS, OTMS, and HDTMS are 1, 8, and 16, respectively. The measured water contact angle of $SiO_2$-$TiO_2$-MTMS, $SiO_2$-$TiO_2$-OTMS, and $SiO_2$-$TiO_2$-HDTMS coated glass under similar conditions is also depicted in Figure 9. It was clear that increasing the alkyl chain length up to C=8 increased the water contact angle, due to the non-polar contribution from alkylsilane. The contact angle value increased with an increase in the alkyl chain length. Coating with long alkyl-chain silane significantly reduced the surface energy of the glass, which was also favorable for enhancing the water-repellent effect.

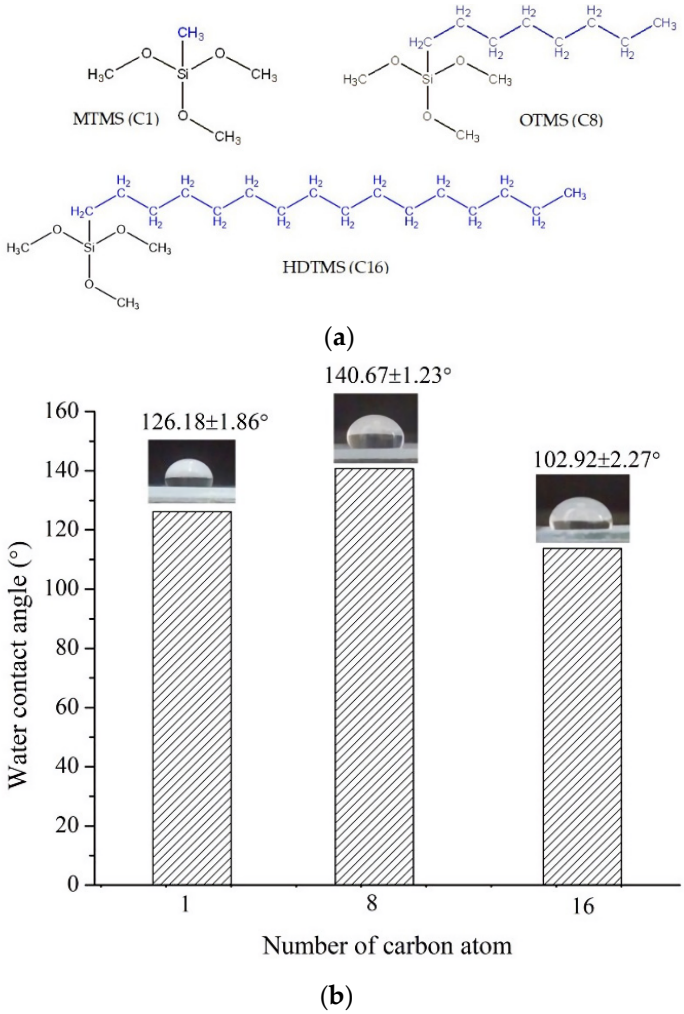


**Figure 9.** (**a**) The molecular structure of MTMS (C1), OTMS (C8), HDTMS (C16), and (**b**) water contact angles, measured on $SiO_2$-$TiO_2$-alkylsilane coated glass samples.

However, the water contact angle of C=16 showed the opposite trend. The measured contact angle was decreased. According to the surface energy, HDTMS (C16) should have lower surface energy than MTMS (C1) and OTMS (C8); therefore, HDTMS should present a higher contact angle than other samples. In fact, coating the glass samples with $SiO_2$-$TiO_2$-HDTMS resulted in the lowest contact angle.

To study the effect of alkyl chain-length silane on hydrophobicity, we characterized the topography of coated glass samples using SEM and AFM. The SEM images of $SiO_2$-$TiO_2$-MTMS, $SiO_2$-$TiO_2$-OTMS, and $SiO_2$-$TiO_2$-HDTMS coated glass samples are shown in Figure 10. The $SiO_2$-$TiO_2$-HDTMS presented a lower surface roughness than $SiO_2$-$TiO_2$-MTMS and $SiO_2$-$TiO_2$-OTMS. The smooth surface of the $SiO_2$-$TiO_2$-HDTMS proved that the long chains of HDTMS did not align vertically on the surface and instead formed collapsed molecules.

### *3.3. The Influence of Surface Roughness on Hydrophobicity*

The profile of the surface roughness was displayed in Figure 11. It showed the AFM images of $SiO_2$-$TiO_2$-MTMS, $SiO_2$-$TiO_2$-OTMS, and $SiO_2$-$TiO_2$-HDTMS. The samples showed that the root mean square (RMS) values were 188 nm for $SiO_2$-$TiO_2$-MTMS, 291 nm for $SiO_2$-$TiO_2$-OTMS, and 29.8 nm for $SiO_2$-$TiO_2$-HDTMS, respectively. An analysis of both showed that the $SiO_2$-$TiO_2$-HDTMS evinced the smoothest surfaces, while $SiO_2$-$TiO_2$-OTMS presented the roughest surfaces. This data supported the results and analysis of SEM images.

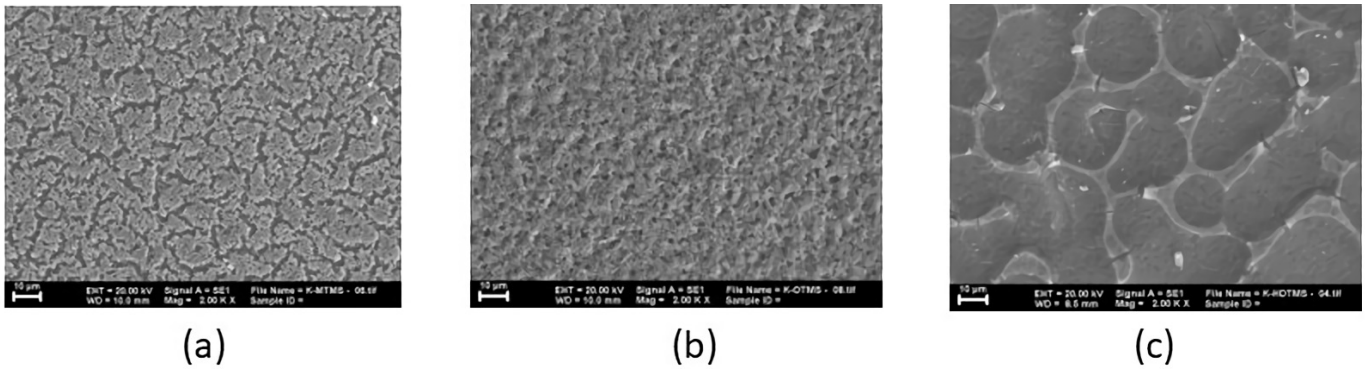


**Figure 10.** The SEM images of (**a**) $SiO_2$-$TiO_2$-MTMS, (**b**) $SiO_2$-$TiO_2$-OTMS, and (**c**) $SiO_2$-$TiO_2$-HDTMS.

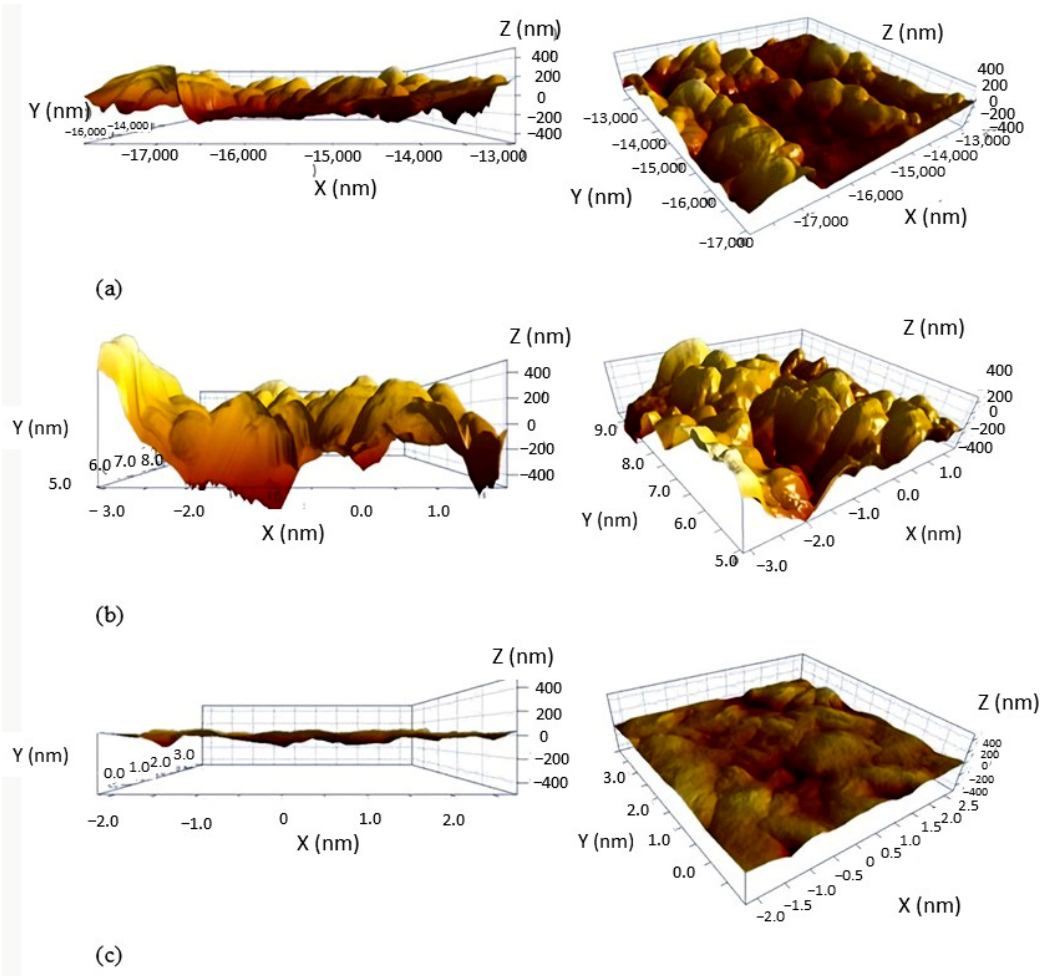


**Figure 11.** The AFM images of (**a**) $SiO_2$-$TiO_2$-MTMS, (**b**) $SiO_2$-$TiO_2$-OTMS, and (**c**) $SiO_2$-$TiO_2$-HDTMS coatings.

On the rough surfaces, there was trapped air that filled the grooves on the surface. When the water dropped onto the surface, entrapped air gave an upward thrust, resulting in an adhesion force toward water droplets. It is not easy for the water to penetrate the solid surface. It will rest on top of the surface and minimize the interaction between the water and the solid. Finally, a hydrophobic surface is generated. The larger area of entrapped air, and the lower the interaction of the water–solid, the higher the hydrophobicity. Consequently, the portion of air trapped in the solid surface is the main factor in controlling hydrophobicity. Figure 12 illustrates the correlation between surface roughness and hydrophobicity.

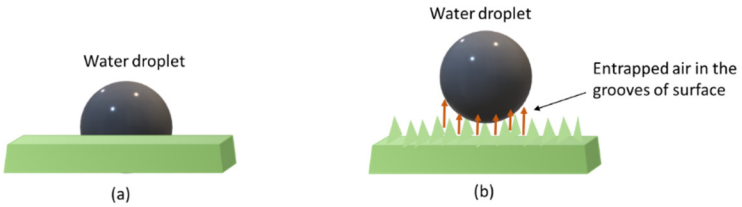


**Figure 12.** A schematic illustration of a water droplet on (**a**) smooth and (**b**) rough surfaces.

AFM images can also identify and determine the orientation of molecules on the surface, which influences the topography of the surface. $SiO_2$-$TiO_2$-MTMS, $SiO_2$-$TiO_2$-OTMS, and $SiO_2$-$TiO_2$-HDTMS films had surface heights of about 100–300, 100–400, and 0–50 nm, respectively. The $SiO_2$-$TiO_2$-MTMS and $SiO_2$-$TiO_2$-OTMS coatings formed self-assembled molecules because the longer the alkyl chain, the greater the height of the coating on the surface. In contrast to $SiO_2$-$TiO_2$-MTMS and $SiO_2$-$TiO_2$-OTMS, $SiO_2$-$TiO_2$-HDTMS demonstrated a low height of surface. It was predicted that HDTMS with a long alkyl chain would create self-assembly disorder. We assumed that most of the molecules formed a collapsed structure on the surfaces. Molecules tended to form a horizontal orientation on the surface. The prediction of the molecule conformation of coatings is displayed in Figure 13. These data were in line with previous research, which stated that collapsed molecules generated smooth surfaces [16].

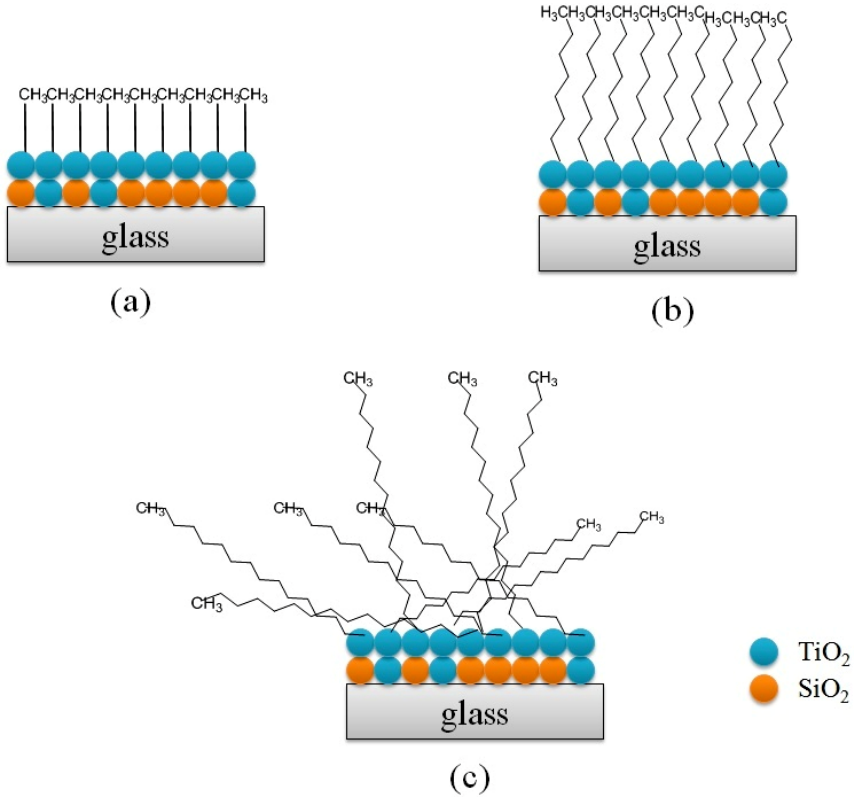


**Figure 13.** The prediction of molecule conformation of (**a**) $SiO_2$-$TiO_2$-MTMS, (**b**) $SiO_2$-$TiO_2$-OTMS, and (**c**) $SiO_2$-$TiO_2$-HDTMS-coated glass.

In the collapsed molecules, the water-surface interaction of $CH_2$ groups was greater than with $CH_3$ groups when the water droplets were sitting on the surface [19,20]. As we know, $CH_2$ groups create higher surface energy than $CH_3$ groups; therefore, the collapsed molecules tended to produce a low contact angle.

### 3.4. The Influence of Coating Technique on Hydrophobic Coatings

Figure 14 shows the influence of the coating technique on the hydrophobicity and surface roughness of coated glass samples. Coatings made by the one-layer technique had a higher contact angle than coatings created by the layer-by-layer technique. This can be attributed to the difference in surface roughness. The higher surface roughness was observed in the one-layer technique. The rougher the surface, the higher the hydrophobicity. In contrast, the layer-by-layer technique created smooth surfaces. The loss of surface roughness could have occurred when the thick coating covered the metal oxide layers [21].

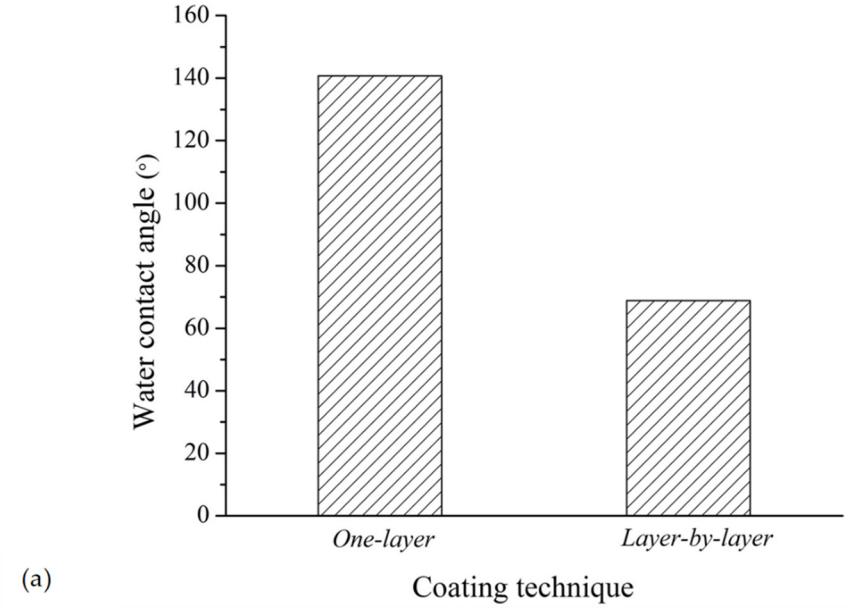


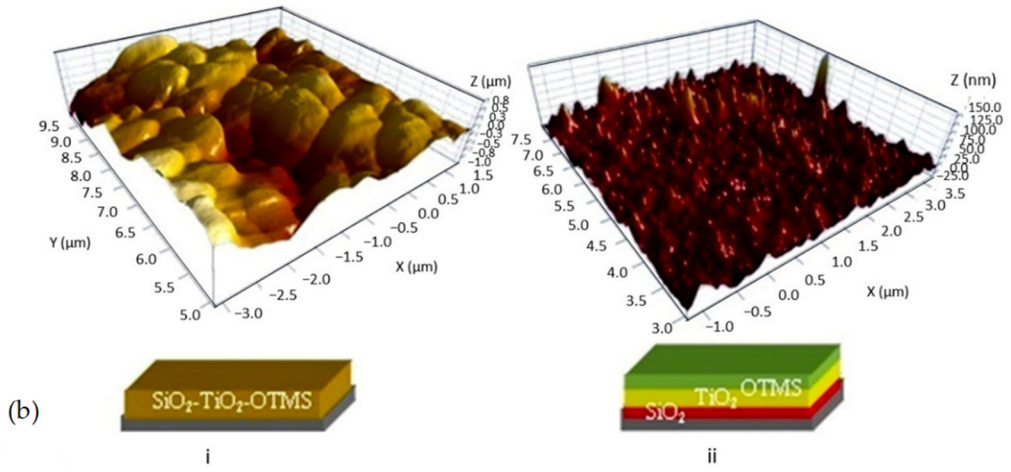


**Figure 14.** (**a**) The correlation between water contact angle and the coating technique of $SiO_2$, $TiO_2$, and OTMS-coated glass. (**b**) The AFM images of $SiO_2$, $TiO_2$, and OTMS-coated glass were prepared using (**i**) one layer and (**ii**) layer-by-layer coating techniques.

### 3.5. Stability of Coatings

Figure 15 displays the stability of coatings undergoing outdoor exposure for four weeks. The hydrophobicity of $SiO_2$-$TiO_2$-MTMS and $SiO_2$-$TiO_2$-HDTMS coatings gradually degraded during outdoor exposure. In contrast, the water-repellent capability of the $SiO_2$-$TiO_2$-OTMS coating was stable for four weeks. The decrease in contact angle was probably due to the absorption of moisture from the atmosphere by the polar –OH bonds

in the surfaces [22]. A similar result was also obtained in our previous research [11]. The stability of $SiO_2$-$TiO_2$-OTMS was predicted because of the contribution made by its surface roughness. The high surface roughness was expected to make it difficult for dirt to adhere.

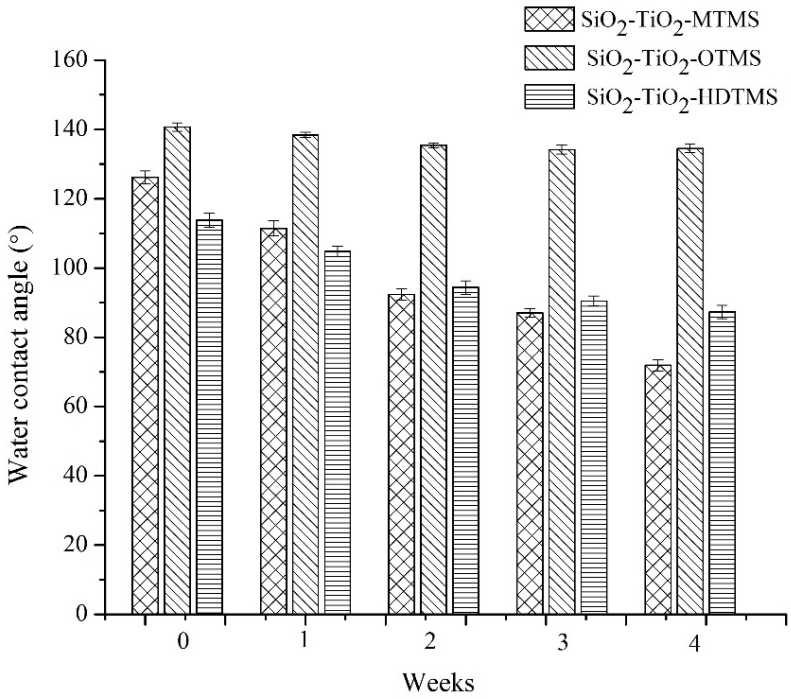


**Figure 15.** The change in the water contact angle of coatings undergoing outdoor exposure for four weeks.

### *3.6. Anti-Dirt Performance of Coatings*

Up to now, there has been no standard procedure for investigating the self-cleaning performance of coatings [2]. Figure 16 shows the difference in the behavior of uncoated glass and coated glass after dirt deposition on their surfaces. On the uncoated glass, a great deal of dirt accumulated on the surface. In contrast, there was no dirt adhering to the highly hydrophobic surface. The very rough surface was predicted to be able to prevent dirt attachment to the coating.

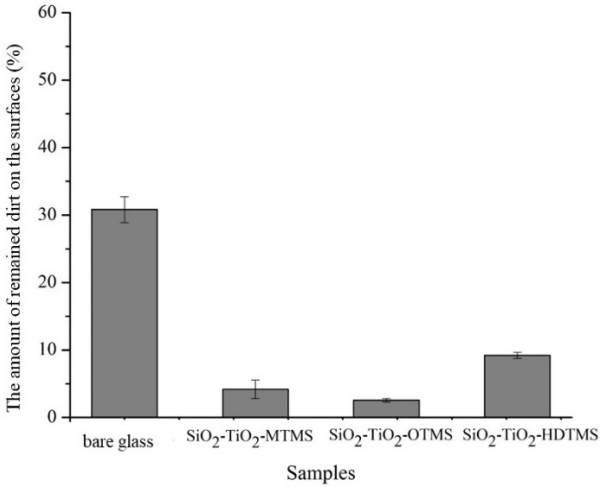


**Figure 16.** The amount of remaining dirt on the $SiO_2$-$TiO_2$-OTMS coated glass surface after the self-cleaning test.

## 4. Conclusions

A highly hydrophobic, anti-dirt, and durable coating was prepared using $SiO_2$-$TiO_2$-alkylsilane through sol-gel deposition and the one-layer coating technique. The use of $SiO_2$ and $TiO_2$ helped to enhance the surface roughness and adhesion strength of the coatings. The longer the alkyl chain length of silane (up to C=8), the higher the hydrophobicity of the coatings. However, the water contact angle decreased when the C=16 formulation of alkylsilane was applied. It was predicted that the surfaces were then composed of disordered molecules. Interestingly, the as-prepared samples demonstrated the anti-dirt accumulation performance on the surfaces, so that no water was needed to clean the surfaces. Further research will focus on the engineering of coatings to maintain the transparency of glass. Based on its high hydrophobicity, durability, and excellent anti-dirt properties, this coating shows promise in many applications.

**Author Contributions:** Conceptualization, A.A.W.; methodology, A.A.W.; software, A.A.W. and M.Z.F.; validation, S.C.W.S. and T.E.P.; formal analysis, A.A.W., M.Z.F., and S.C.W.S.; investigation, A.A.W., M.Z.F., S.C.W.S. and T.E.P.,; resources, A.A.W. and T.A.B.; data curation, A.A.W. and T.E.P.; writing—original draft preparation, A.A.W.; writing—review and editing, A.A.W., M.Z.F. and S.C.W.S.; visualization, A.A.W. and T.A.B.; supervision, A.A.W.; project administration, A.A.W. and T.A.B.; funding acquisition, A.A.W. All authors have read and agreed to the published version of the manuscript.

**Funding:** This research was funded by the Ministry of Research, Technology and Higher Education, Indonesia, through the PD Grant of Universitas Airlangga, No. 4/AMD/E1/KP.PTNBH/2020 and 788/UN3.14/PT/2020.

**Data Availability Statement:** Not applicable.

**Acknowledgments:** The authors are grateful to the Department of Chemistry in the Faculty of Science and Technology, Universitas Airlangga, for the laboratory facilities provided.

**Conflicts of Interest:** The authors declare no conflict of interest. The funders had no role in the design of the study; in the collection, analyses, or interpretation of data; in the writing of the manuscript; or in the decision to publish the results.

## References

1. Quan, Y.Y.; Zhang, L.Z.; Qi, R.H.; Cai, R.R. Self-cleaning of Surfaces: The role of surface wettability and dust types. *Sci. Rep.* **2016**, *6*, 38239. [CrossRef]
2. Kumar, D.; Wu, X.; Fu, Q.; Ho, J.W.C.; Kanhere, P.D.; Li, L.; Chen, Z. Hydrophobic sol-gel coatings based on polydimethylsiloxane for self-cleaning applications. *Mater. Des.* **2015**, *86*, 855–862. [CrossRef]
3. Zhang, Z.H.; Wang, H.J.; Liang, Y.H.; Li, X.J.; Ren, L.Q.; Cui, Z.Q.; Luo, C. One-step fabrication of robust superhydrophobic and superoleophilic surfaces with self-cleaning and oil/water separation function. *Sci. Rep.* **2018**, *8*, 3869. [CrossRef]
4. Norgaard, A.W.; Hansen, J.S.; Sorli, J.B.; Levin, M.; Wolkoff, P.; Nielsen, G.D.; Larsen, S.T. Pulmonary Toxicity of Perfluorinated Silane-Based Nanofilm Spray Products: Solvent Dependency. *Toxicol. Sci.* **2013**, *137*, 180–188. [CrossRef]
5. Pan, G.; Zhou, Q.; Luan, X.; Fu, Q.S. Distribution of perfluorinated compounds in lake taihu (China): Impact to human health and water standards. *Sci. Total Environ.* **2014**, *487*, 778–784. [CrossRef]
6. Song, J.; Rojas, O.J. Approaching super-hydrophobicity from cellulosic materials: A review. *Nord. Pulp Pap. Res. J.* **2013**, *28*, 216–238. [CrossRef]
7. Lin, J.; Chen, H.; Fei, T.; Zhang, J. Highly transparent superhydrophobic organic-inorganic nanocoating from the aggregation of silica nanoparticles. *Colloids Surfaces A Physicochem. Eng. Asp.* **2013**, *421*, 51–62. [CrossRef]
8. Hwang, J.; Ahn, Y. Fabrication of superhydrophobic silica nanoparticles and nanocomposite coating on glass surfaces. *Bull. Korean Chem. Soc.* **2015**, *36*, 391–394. [CrossRef]
9. Petcu, C.; Purcar, V.; Spătaru, C.; Alexandrescu, E.; Şomoghi, R.; Trică, B.; Niţu, S.G.; Panaitescu, D.M.; Donescu, D.; Jecu, M.L. The influence of new hydrophobic silica nanoparticles on the surface properties of the films obtained from bilayer hybrids. *Nanomaterials* **2017**, *7*, 47. [CrossRef]
10. Widati, A.A.; Nuryono, N.; Kartini, I.; Martino, N.D. Silica-methyltrimethoxysilane based hydrophobic coatings on a glass substrate. *J. Chem. Technol. Metall.* **2017**, *52*, 1123–1128.
11. Widati, A.A.; Nuryono, N.; Aryanti, D.P.; Wibowo, M.A.; Kunarti, E.S.; Kartini, I.; Rusdiarso, B. Preparation of water repellent layer on glass using hydrophobic compound modified rice hull ash silica. *Indones. J. Chem.* **2018**, *18*, 587–593. [CrossRef]

12. Ramírez-García, R.E.; González-Rodríguez, J.A.; Arroyo-Ortega, M.; Pérez-García, S.A.; Licea-Jiménez, L. Engineered $TiO_2$ and $SiO_2$-$TiO_2$ films on silica-coated glass for increased thin film durability under abrasive conditions. *Int. J. Appl. Ceram. Technol.* **2017**, *14*, 39–49. [CrossRef]
13. Liu, S.; Liu, X.; Latthe, S.S.; Gao, L.; An, S.; Yoon, S.S.; Liu, B.; Xing, R. Self-cleaning transparent superhydrophobic coatings through simple sol-gel processing of fluoroalkylsilane. *Appl. Surf. Sci.* **2015**, *351*, 897–903. [CrossRef]
14. Hu, Y.; Wang, Y.; Yang, H. TEOS/Silane-Coupling Agent Composed Double Layers Structure: A Novel Super-hydrophilic Surface. *Energy Procedia* **2015**, *75*, 349–354.
15. Spataru, C.I.; Purcăr, V.; Donescu, D.; Ghiurea, M.; Cinteză, O.; Miclăuš, T. Preparation of hydrophobic surface based on hybrid silica films by sol-gel process. *UPB Sci. Bull. Ser. B Chem. Mater. Sci.* **2013**, *75*, 117–128.
16. Tang, Z.; Li, H.; Hess, D.; Breedveld, V. Effect of chain length on the wetting properties of alkyltrichlorosilane coated cellulose-based paper. *Cellulose* **2016**, *23*, 1401–1413. [CrossRef]
17. Dong, S.; Wang, Z.; Wang, Y.; Bai, X.; Fu, Y.Q.; Guo, B.; Tan, C.; Zhang, J.; Hu, P. Rol-to-roll manufacturing of robust superhydrophobic coating on metallic engineering materials. *ACS Appl. Mater. Interfaces* **2018**, *10*, 2174–2184. [CrossRef] [PubMed]
18. Prakash, P.; Satheesh, U.; Devaprakasam, D. Study of High Temperature Thermal Behavior of Alkyl and Perfluoroalkylsilane Molecules Self-Assembled on Titanium Oxide Nanoparticles. *arXiv* **2014**, arXiv:1409.6823.
19. Farzaneh, M.; Kulinich, S.A. Hydrophobic properties of surface coated with fluoroalkylsilane and alkylsiloxane monolayers. *Surf. Sci.* **2004**, *573*, 379–390.
20. Kulinich, S.A.; Farzaneh, M. Alkylsilane self-assembled monolayers: Modeling their wetting characteristics. *Appl. Surf. Sci.* **2004**, *230*, 232–240. [CrossRef]
21. Hu, J.; Pan, C.; Li, H.; Shen, P.; Sun, H.; Duan, H.; Lanza, M. Improvement of the electrical contact resistance at rough interfaces using two dimensional materials. *J. Appl. Phys.* **2015**, *118*, 215301. [CrossRef]
22. Kavale, M.S.; Mahadik, D.B.; Parale, V.G.; Wagh, P.B.; Gupta, S.C.; Rao, A.V.; Barshilia, H.C. Optically transparent, superhydrophobic methyltrimethoxysilane based silica coatings without silylating reagent. *Appl. Surf. Sci.* **2011**, *258*, 158–162. [CrossRef]